

Design of a fuzzy safety margin derivation system for grip force control of robotic hand in precision grasp task

International Journal of Advanced
Robotic Systems

May-June 2021: 1–12

© The Author(s) 2021

Article reuse guidelines:

sagepub.com/journals-permissions

DOI: 10.1177/17298814211018055

journals.sagepub.com/home/arx



Canfer Islek^{ORCID} and Ersin Ozdemir^{ORCID}

Abstract

In this study, the aim was to grasp and lift an unknown object without causing any permanent change on its shape using a robotic hand. When people lift objects, they add extra force for safety above the minimum limit value of the grasp force. This extra force is expressed as the “safety margin” in the literature. In the conducted study, the safety margin is minimized and the grasp force was controlled. For this purpose, the safety margin performance of human beings for object grasping was measured by the developed system. The obtained data were assessed for a fuzzy logic controller (FLC), and the fuzzy safety margin derivation system (SMDS) was designed. In the literature, the safety margin rate was reported to vary between 10% and 40%. To be the basis for this study, in the experimental study conducted to measure the grip performance of humans, safety margin ratios ranging from 9% to 20% for different surface friction properties and different weights were obtained. As a result of performance tests performed in Matlab/Simulink environment of FLC presented in this study, safety margin ratios ranging from 8% to 21% for different surface friction properties and weights were obtained. It was observed that the results of the performance tests of the developed system were very close to the data of human performance. The results obtained demonstrate that the designed fuzzy SMDS can be used safely in the control of the grasp force for the precise grasping task of a robot hand.

Keywords

Fuzzy logic, grasping force control, precision grasp, robotic hand, safety margin

Date received: 24 February 2021; accepted: 27 April 2021

Topic Area: Robot Manipulation and Control

Topic Editor: Marco Ceccarelli

Associate Editor: Erwin-Christian Lovasz

Introduction

Nowadays, different robot applications are seen in almost every area of life. Robots are in the future plans of countries. In Japan, where the robot industry has been developed, the slogan of “A robot for every home” has become the goal of the country.

Robots are interdisciplinary devices that consist of electronic and mechanical units for various physical skills to mimic the functions and behaviors of living creatures and have the abilities of sensing and performing tasks with programmable algorithms. It is expected that a robot can perform tasks such as grasping and lifting objects by

controlling its hands, arms, and fingers, just like a human. Grasping was divided into two main classes by Cutkosky,¹ power grasp and precision grasp, distinguished by the

Faculty of Engineering and Natural Sciences, Department of Electrical and Electronic Engineering, Iskenderun Technical University, İskenderun, Hatay, Turkey

Corresponding author:

Ersin Ozdemir, Faculty of Engineering and Natural Sciences, Department of Electrical and Electronic Engineering, Iskenderun Technical University, 31200 İskenderun, Hatay, Turkey.

Email: ersin.ozdemir@iste.edu.tr



Creative Commons CC BY: This article is distributed under the terms of the Creative Commons Attribution 4.0 License (<https://creativecommons.org/licenses/by/4.0/>) which permits any use, reproduction and distribution of the work without

further permission provided the original work is attributed as specified on the SAGE and Open Access pages (<https://us.sagepub.com/en-us/nam/open-access-at-sage>).



Figure 1. The two-finger precision grasp.

structural characteristics of the object to be grasped, conditions of the fingers, and the nature of grasp task. Powerful grasp is the grasp class, where safety and stability are important. Precision grasp, on the other hand, is the grasp class, where skill and precision are important.

In this study, soft fingertip contact model and two-finger precision grasp model, where thumb and index finger grasp was used, were considered as in Figure 1.

For a robotic hand, grasping and manipulation is a complex task containing a movement plan in terms of kinematic and force control in both statics and dynamics.² The reason why this task is complex is due to the problems associated with the geometry, durability, hardness, and surface properties of the object to be gripped. The analytical modeling problems related to these issues are classified by Cutkosky¹ as follows:

- Geometry
- Kinematic
- Dynamic
- Constitutive relations.

The friction interaction between the fingertips and the surfaces of the objects to be gripped is one of the important problems that must be solved in the class of problems caused by constitutive relations. In the context of Coulomb friction law, the ability of people to grasp and lift objects depends on the friction force between the fingertips and the surfaces of the object. The grip force applied in an uncontrolled way in precise grip task can lead to permanent deformation such as cracking and breaking the object. Grip force applied less due to the concern of causing permanent deformation may cause the object to fall. This shows the necessity of controlling the grip force in grip task of a robotic hand.

There are many studies on the control of robotic hand force in the literature. Before the studies on robotic hand-grip, human grip skills were studied and a significant experimental medical literature has been formed for the grip skills of human hand.³ Tremblay et al.⁴ developed an approach that can control grip force by determining the small and initial slips between the gripped object and finger surface of the robotic hand before the gross slip. In their study, Tremblay and Cutkosky⁵ proposed a grip force control strategy and optimal prediction method of friction coefficient with the perception of small local slips that occur before gross slip between the object and finger for precise grasping and manipulation task of slippery or fragile objects with a robotic hand. Dubey et al.⁶ proposed a “force relaxation” algorithm that will provide grasping an unknown object with an optimum force through a fuzzy logic-based control method and the controller system they presented. Glossas and Aspragathos⁷ presented a fuzzy logic-based control method for grasping unknown, fragile, and sensitive objects with a minimum force for a robotic grasping system with two fingers. Domínguez-López et al.⁸ presented a neural fuzzy-based control method and hybrid controller system for an optimum grip and force control without damaging or slipping the unknown object like weight and surface roughness. In their study, Maeno et al.⁹ proposed an approach to grasp and lift an object without knowing its weight and coefficient of friction (CoF) by not causing permanent deformation and slipping with trying to estimate the CoF between two surfaces by analyzing the tensile distribution on the surface of elastic finger shape sensor via finite-element method. Ikeda et al.¹⁰ suggested a visual-based grip force control method on the basis of stick-slip friction model without the need of knowing the CoF in the grip of a soft object. Koda and Maeno¹¹ presented master-slave control method for force control and gripping an object with unknown surface friction properties using Coulomb friction law and feedback from the partial slip sensor they developed. In the fuzzy logic-based control method presented by O’Toole et al.,¹² a fuzzy sliding mode controller was proposed for gripping soft and fragile objects with a minimum contact force and without slipping. Ho and Hirai¹³ focused on stick-slip transition during sliding using Coulomb friction law and finite-element analysis on a sensor designed for the stick-slip friction model. Yuan et al.¹⁴ focused on determining normal, shear, and torsion forces with a tactile sensor for the task of a robotic hand to grasp an object and determining the start of partial local slip formed before the gross slip that may occur between the finger and the gripped object. In their studies, Lu et al.¹⁵ formulized contact force to be equal or smaller than the maximum contact force using Coulomb friction model for the optimization of contact force and applied. In their study conducted using slip sensor, Morita et al.¹⁶ presented the grip force control method in which the minimum grip force was estimated on the basis of Coulomb friction law when the slip is sensed

between the robotic finger and object. Pettersson-Gull and Johansson¹⁷ presented a grip force control technique based on the principle of increasing normal force until the relative movement between the finger stopped during sliding of the object. Calandra et al.¹⁸ taught the neural network to grasp behaviors with multiple grasping trials in an action-conditional model they presented for grip force control using visual and tactile data.

The minimum limit value of a normal force to grip and lift an object can be calculated theoretically by Coulomb's friction law. The maximum grip force value that will not cause permanent deformation on the object can be theoretically calculated with Hook's law. However, these limit values are not very useful in practice. The surfaces of the objects to be grasped and lifted are not homogeneous due to different roughness distribution and the foreign materials such as dirt, humidity, and oil under natural conditions. The weight and strength values of the object during grasping are also unknown properties. Under the effects of combined force, controlling grip force for the objects having nonhomogeneous surfaces and unknown properties results in a complex problem. In a precise grip task of a robotic hand, it is quite difficult to prepare a mathematical model in which the optimum grip force can be calculated.

While people grasp and lift objects, they add extra force for safety over the minimum limit value of normal force that can be calculated with Coulomb's friction law.^{19–21} In the literature, this extra force is often expressed as "safety margin." A safety margin is an extra force applied in a controlled manner. The basic element that causes permanent deformation in the object to be grasped is the uncontrolled extra force applied by the fingers. In this study, the control of grip force with optimum safety margin was aimed for precision grasp task of a robotic hand.

There is no mathematical model for how much the safety margin should be under what conditions. However, people can precisely grasp and lift any object without knowing its properties with optimum safety margin under natural conditions. This skill is an ability that people have gained experimentally since infancy. Tremblay and Cutkosky⁵ stated that the safety margin rate varies between 15% and 100% and accepted the safety margin rate in their study as 20%. Wettels et al.²² applied a 20% safety margin rate on the estimated slip point. In some conducted studies, safety margin was stated to vary between 10% and 40%.^{23–25} Hiramatsu et al.,²⁶ in their experimental study, reported that the safety margin ranged from 40% to 50% when lifting objects weighing 100 g or more. In this study, fuzzy logic method from flexible calculation methods was used to control grip force with optimum safety margin. In the precise grip, a fuzzy logic controller (FLC) was designed using safety margin data applied by humans for objects with different surface characteristics and different weights. The designed fuzzy logic controlled is called the fuzzy safety margin derivation system (SMDS). In this way, safety

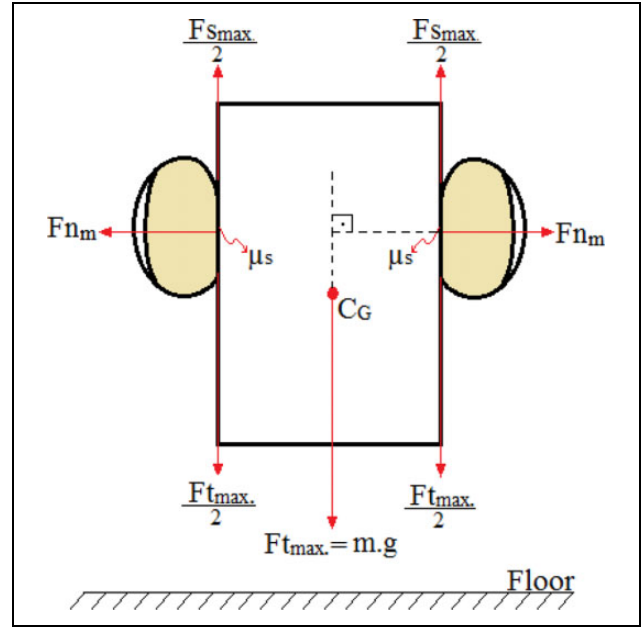


Figure 2. Lifting an object with two fingers.²⁷

margin calculation was conducted in precise grip for different surface properties and different weights.

Material and method

To grasp and lift an object, the object surface should hold onto the grip surface of the fingers. The main element keeping the object hanging between the fingers without slipping and falling is the friction force. Hold conditions of the objects to be grasped and lifted on the grasping surface of the fingers are explained with Coulomb's friction equation in equation (1)

$$F_{s_{\max}} = F_n \cdot \mu_s \quad (1)$$

In equation (1), F_n (normal force) refers to the grip force applied by the finger and μ_s is the coefficient of static friction between the finger surface and object surface. $F_{s_{\max}}$ expresses the maximum static friction force preventing the object to slip. The case of grasping and lifting an object with two fingers is shown in Figure 2. F_{n_m} shown in Figure 2 is the normal force (F_n) value plus S_m (safety margin) applied by each finger when lifting event occurs. F_{n_m} can be expressed as in equation (2).

$$F_{n_m} = F_n + S_m \quad (2)$$

where $F_{t_{\max}}$ is the maximum tangential force value expressing the total weight of the object. Since $F_{t_{\max}}$ value would be equal to $F_{s_{\max}}$, equation (1) can be expressed as in equation (3) in accordance with the case in Figure 2

$$F_{t_{\max}} = 2 \cdot F_n \cdot \mu_s \quad (3)$$

Using equations (2) and (3), the equation of the maximum tangential force value (total weight of the object)

from the time of lifting the object is expressed as in equation (4). From this point, safety margin equation given in equation (5) can be obtained

$$F_{t_{\max}} = 2 \cdot \mu_s \cdot (F_{n_m} - S_m) \quad (4)$$

$$S_m = F_{n_m} - (F_{t_{\max}} / 2 \cdot \mu_s) \quad (5)$$

In this study, slips that take place during grip-lift process are evaluated. Equation (3) was written based on the Coulomb friction equation that can be written for each slip point that occurs during the grip-lift process. In this case, equation (3) is expressed as in equation (6) in terms of local values occurring at slip points

$$F_{t_s} = 2 \cdot F_{n_s} \cdot \mu_{ss} \quad (6)$$

where F_{t_s} in equation (6) refers to the local tangential force (local weight), F_{n_s} denotes the local normal force at the slip point, and μ_{ss} expresses the local static CoF calculated when the slip occurs. In this case, $F_{t_{\max}}$, F_n , F_{n_m} , S_m , and μ_s represent the global values at the moment of lifting the object. If the applied force (grip force) is not enough to lift the total weight of the object, a slip event occurs. When the object is pulled up, the current normal force must be increased so that this slip does not occur again. When the object is pulled up again, if the increased normal force is not sufficient to lift the object, the slip will occur again. This process will continue until the point where the total normal force is sufficient to lift the total weight of the object.

In this study, an approach has been introduced in which the tangential force value formed at each slip point is accepted as the actual weight of the object. Because the actual weight of the object to be gripped is unknown. Thus, by adding a safety margin to each slip point, the object is tried to be lifted. The force added on the current normal force for each slip point is named S_{m_s} (local safety margin which added for the slip point). For the calculation of S_{m_s} , SMDS with fuzzy logic has been designed. For the expert knowledge that will form the knowledge base in the design of SMDS, safety margin data applied by people according to changing conditions are needed.

Precise gripping-lifting experiments were conducted by Islek and Özdemir²⁷ with an experimental setup seen in Figure 3, whose weight and surface properties can be changed. There is a load cell available at the base of the experimental setup to detect the weight of the object. In addition, load cells are mounted on the gripping surfaces for detecting grip force. Islek and Özdemir²⁷ conducted their experiments with four different weights between 300 gf and 900 gf and five different coefficients of static frictions between 0.07 and 0.75. They obtained optimum safety margin values and safety margin percentage rates according to varying weights and surface properties as a result of precise gripping-lifting experiments conducted with 14 people, as seen in Figure 4.

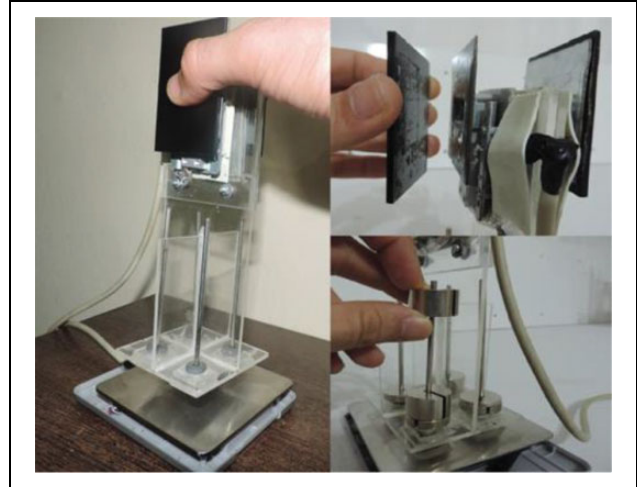


Figure 3. Experimental setup.

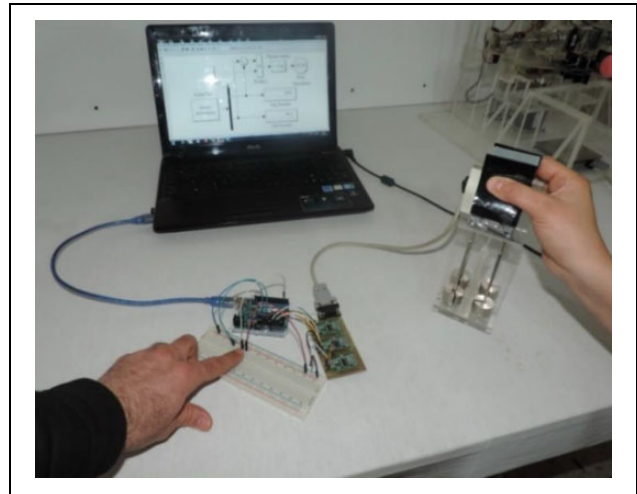


Figure 4. Precise gripping-lifting experiment.

In the conducted precise gripping-lifting experiments, five experiments were carried out with each of 14 people (E1–E14) for each measurement point. In this way, 70 safe grasp force (F_{n_m}) data were obtained for each measurement point. Safety margins of 70 data were then measured using equation (5). For example, safety margins calculated for 300 gf weight and 0.55 coefficient of static friction are presented in Table 1.

From 70 safety margin data calculated, the 14 data with the lowest values were determined. Then, weighted averages of these 14 data were calculated. While calculating weighted averages, the repetition numbers of each of 14 data in 70 data were determined as weight (w). For example, the weighted average calculated for 300 gf weight and 0.55 coefficient of static friction can be seen in Table 2.

As given in Table 2, optimum safety margin data for human grip performance were obtained with the calculation of weighted averages for each weight and coefficient of

Table 1. Weighted average calculated for 300 gf and 0.55 coefficient of static friction.

	Experiments (300 gf–0.55 μ_s)													
	E1	E2	E3	E4	E5	E6	E7	E8	E9	E10	E11	E12	E13	E14
S_m (gf)	96	67	12	130	62	92	29	144	141	92	82	76	22	130
	97	35	49	136	43	93	35	150	151	99	90	86	57	141
	100	43	36	141	73	94	76	156	133	109	93	117	25	147
	106	96	25	141	25	114	79	177	122	116	112	91	78	157
	118	96	100	137	92	123	81	167	143	132	129	134	89	148

Table 2. Weighted average calculated for 300 gf and 0.55 coefficient of static friction.

w	1	1	1	1	1	1	1	1	1	2	2	1	3	2	1	Weighted average
S_m	12	22	29	36	49	57	62	67	35	43	73	25	76	78		46

Table 3. Obtained optimum safety margins.

S_m (gf)	μ_s	$F_{t_{max}}$ (gf)			
		300	500	700	900
	0.75	33	51	81	120
	0.55	46	70	110	165
	0.28	71	105	160	247
	0.14	111	190	OL	OL
	0.07	174	OL	OL	OL

OL: over-the-limit.

Table 4. Obtained optimum safety margin rates.

$S_m\%$	μ_s	$F_{t_{max}}$ (gf)			
		300	500	700	900
	0.75	16	15	17	20
	0.55	17	15	17	20
	0.28	13	12	13	15
	0.14	11	10	OL	OL
	0.07	9	OL	OL	OL

OL: over-the-limit.

static friction. Safety margin percentage rate ($S_m\%$) values were calculated using equation (7) for optimum safety margins obtained for each measurement point. Obtained S_m data can be seen in Table 3 and $S_m\%$ data can be seen in Table 4.

$$S_m\% = [(2 \cdot \mu_s \cdot S_m) / F_{t_{max}}] \cdot 100 \quad (7)$$

In Tables 3 and 4, data points indicated with “OL” (over-the-limit) are the points where the measurement limits of the load cells are located on the experimental setup in Figure 3. The label value of the load cells used is 2 kg. Load cells were loaded with at most 55% (3100 gf) above the label value. Decimal results found by obtaining safety margin data and safety margin rates were rounded to the nearest integer.

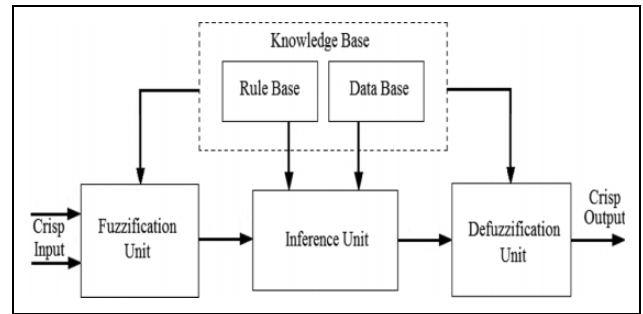


Figure 5. General structure of FLC. FLC: fuzzy logic controller.

Fuzzy logic

The classical logic, also called Aristo logic used in computer systems, is based in the principle that a value is either “present (1)” or “absent (0).” In fuzzy logic, it is accepted that there may be values among these limits. Fuzzy logic systems process inputs consisting of linguistic rules to produce an output.²⁸ Fuzzy logic, first introduced by Zadeh,²⁹ is a method that can model a specialist’s reasoning and decision-making features with algorithms. Fuzzy logic is successfully used in industrial applications, where uncertainty is high and it is hard to find a complex and mathematical model.^{30–32}

Design of the safety margin derivation system

SMDS designed in this study was designed in Matlab R2013a/fuzzy logic toolbox environment. Simulations of SMDS were carried out in Matlab R2013a/Simulink environment. The presented SMDS has the FLC structure, as shown in Figure 5.

The input information taken from a system controlled in a FLC is converted into linguistic symbolic variables depending on a membership function by fuzzy process.^{33,34} Fuzzification unit is fuzzified by intersecting data clusters determined by membership functions. The rule base is the unit in which experts’ decision-making skills are imitated.



Figure 6. Input and output variables of SMDS.

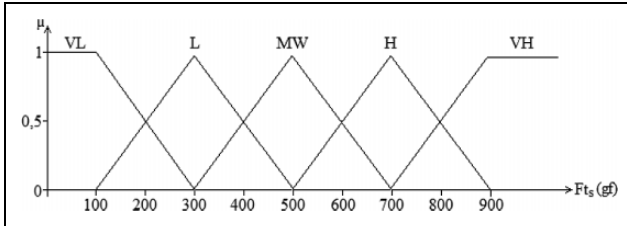


Figure 7. Membership functions of Ft_s input variable.

In the rule base, the relationship between variables consisting of linguistic expressions is coded as IF - THEN rules. The main task of the database is to present the membership and rule table information required for fuzzification, inference, and defuzzification operations to the use of other units of FLC.

In the design of SMDS presented in this study, min-max Mamdani extraction method was used.³⁵ In order for the fuzzy results obtained from fuzzy derivation unit to be used by a controlled system, they need to be converted to a clear or pure number. The center of gravity method was determined as the defuzzification method of SMDS. This method is the most used method among the defuzzification methods.³⁶

Input and output variables of safety margin derivation system

The designed SMDS calculates a local safety margin (Sm_s) for the control of grip force at each slip point. Sm_s value for a slip point is the definitive output of fuzzy function based on local normal force (Fn_s) and local tangential force (Ft_s) values. Thus, as seen in Figure 6, the input variables of SMDS are defined as Fn_s and Ft_s , while the output variable was defined as Sm_s .

Fuzzy cluster of membership function for inputs

Triangle and trapezoid membership functions are used for the input variables of SMDS. As seen in Figure 7, five fuzzy clusters and membership functions were determined between the range of 0–900 gf for Ft_s value.

Linguistic expressions and definition range of fuzzy clusters of Ft_s input variable are defined as: VL (very light): [0, 0, 100, 300]; L (light): [100, 300, 500]; MW (medium-weight): [300, 500, 700]; H (heavy): [500, 700, 900]; and VH (very heavy): [700, 900, $+\infty, +\infty$]. For Fn_s , which is an input variable, seven fuzzy clusters and membership functions were determined in the range of 0–2800 gf, as shown in Figure 8.

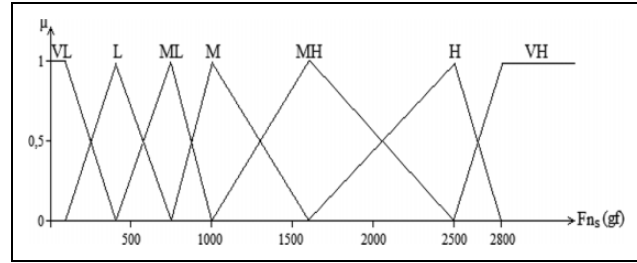


Figure 8. Membership functions of Fn_s input variable.

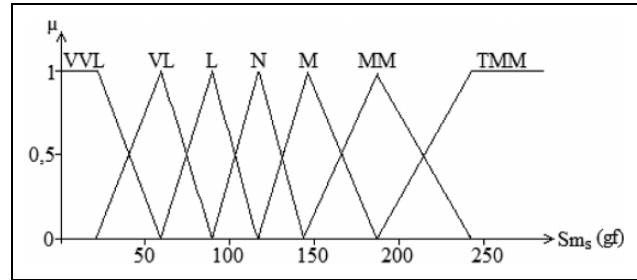


Figure 9. Membership functions of Sm_s output variable.

Linguistic expressions and definition ranges of fuzzy clusters of Fn_s input variable are defined as: VL (very low): [0, 0, 100, 400]; L (low): [100, 400, 750]; ML (medium low): [400, 750, 1000]; M (medium): [750, 1000, 1600]; MH (medium high): [1000, 1600, 2500]; H (high): [1600, 2500, 2800]; and VH (very high): [2500, 2800, $+\infty, +\infty$].

Fuzzy cluster of membership function for outputs

To determine the membership functions of Sm_s , which is the output variable of SMDS and their definition ranges, the data in Tables 3 and 4 were used. Using 15 weighted average values obtained according to different weights and surface properties related to human performance, seven fuzzy clusters and membership functions were determined, as seen in Figure 9. Trapezoid and triangular membership functions were used as membership functions.

Linguistic expressions and definition ranges of the fuzzy clusters of Sm_s output variable were defined as: VVL (very very little): [0, 0, 22, 60]; VL (very little): [22, 60, 90]; L (a little): [60, 90, 117]; N (normal): [90, 117, 147]; M (more): [117, 147, 187]; MM (much more): [147, 187, 243]; and TMM (too much more): [187, 243, $+\infty, +\infty$].

Formation of fuzzy rule base

After obtaining membership functions by fuzzification input and output variables, fuzzy rule base was formed. The relationship between the input variables and output variables expressed the rule statements as: "If Ft_s is MW and Fn_s is MH, then Sm_s is MM." Thus, the rule base consisting of 35 rule statements was derived. The rule table of the input and output variables can be seen in Table 5.

The fuzzy rule base regulating the relationship between the input and output variables was prepared using Matlab/

Table 5. Rule table.

Sm_s	Fn_s							
	VL	L	ML	M	MH	H	VH	
Ft_s	VL	VVL	VVL	VVL	VL	VL	N	N
	L	VVL	VL	L	L	M	MM	MM
	MW	VVL	VL	L	N	MM	MM	TMM
	H	VVL	L	N	N	MM	TMM	TMM
	VH	VVL	L	M	M	TMM	TMM	TMM

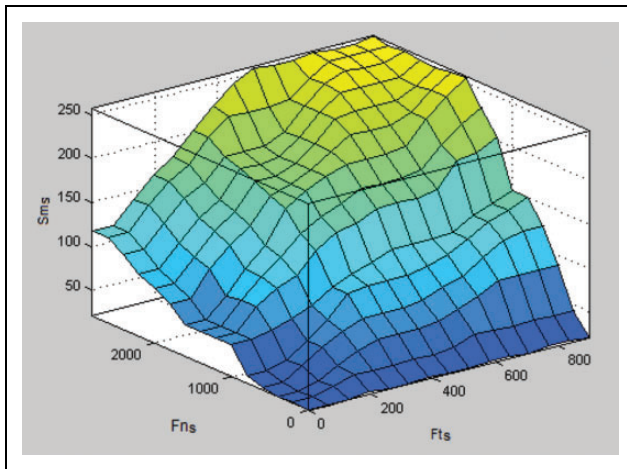


Figure 10. Control surface graph of SMDS. SMDS: safety margin derivation system.

fuzzy rule editor. In Figure 10, the graph of control surface obtained with Matlab/fuzzy surface viewer of the fuzzy rule base of SMDS is shown.

Study and findings

The CoF shown in Figure 11 refers to μ_{ss} . In the prepared model, it was assumed that the surface of the gripped object was homogeneous, and accordingly, CoF value was the same at all slip points. Ten different grip scenarios of up to 900 gf were tested for 10 different CoF values between 0.07 and 0.75. For the beginning, the initial value of grip force was determined as 20 gf. The initial value is also the first Fn_s value.

Ft_s value is obtained using equation (6). By entering Fn_s and Ft_s values into SMDS, local safety margin (Sm_s) is calculated. For each Sm_s value, safety margin percentage is calculated using equation (7). New input values for SMDS are obtained by calculating next Fn_s and Ft_s values by adding the obtained Sm_s value to the previous Fn_s value. This process continues until the grip force reaches to 2800 gf or object weight reaches to 900 gf. By recording all data calculated during the gripping process, the graphs shown in Figures 12 and 13 were obtained. While recording the data, the obtained decimal results were rounded to the nearest integer. When the graph in Figure 12 is examined, it is seen that almost the same Sm_s values are produced for a certain period of time depending on CoF value from the beginning of the simulation. This time period increased as the CoF value decreased (as the slippery property increased). Sm_s

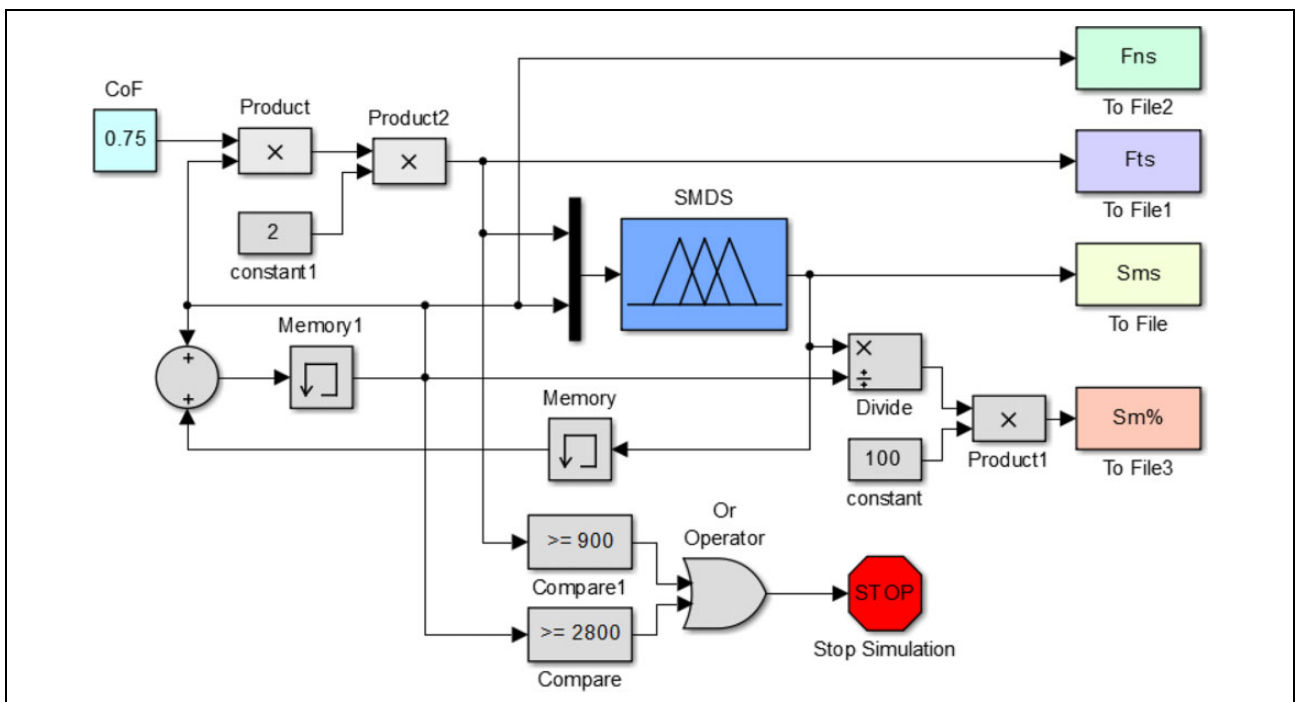


Figure 11. Matlab/Simulink model for gripping performance of SMDS. SMDS: safety margin derivation system.

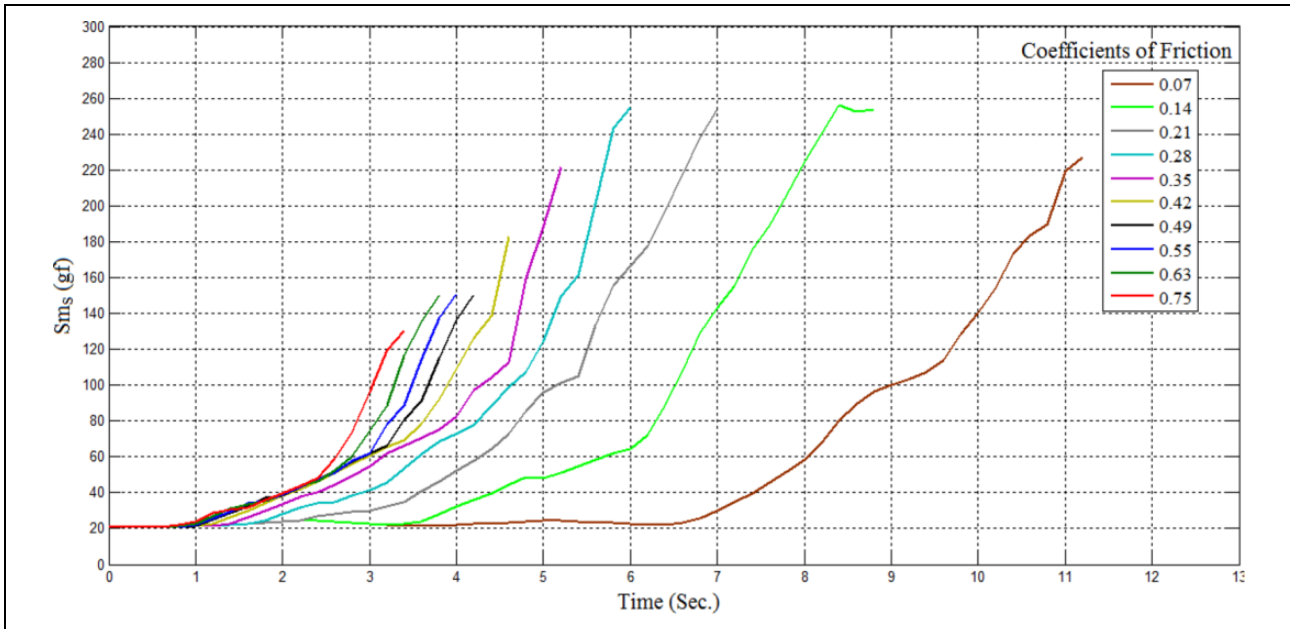


Figure 12. Sm_s derivation performance graph of SMDS. SMDS: safety margin derivation system.

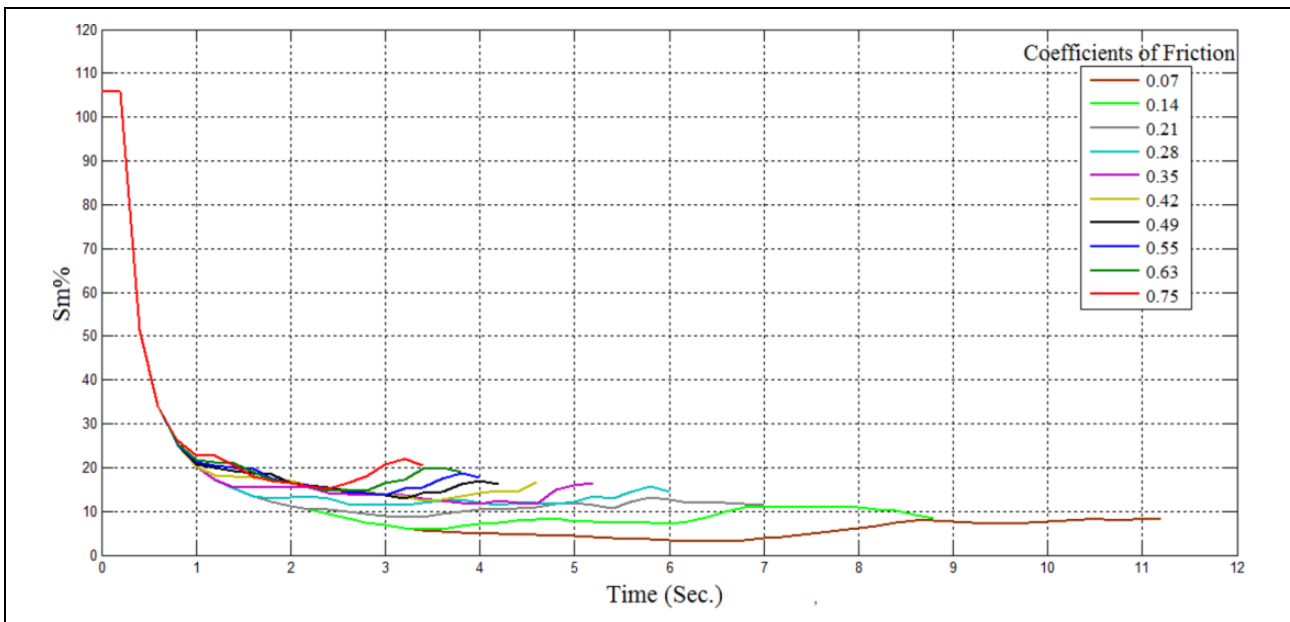


Figure 13. $Sm\%$ derivation performance graph of SMDS. SMDS: safety margin derivation system.

value was found to increase after a certain Fn_s and Ft_s values depending on CoF value.

When the graph in Figure 13 is examined, it is seen that the $Sm\%$ values which were very high at the beginning decreased rapidly and minimized below the 20% levels. As the slipperiness increased, lower $Sm\%$ values were obtained. The lowest $Sm\%$ value was recorded as 3% at 0.07 CoF value. In the sample table given in Table 6, the

Table 6. Sample simulation data obtained from SMDS.

Time (s)	0	0.2	0.4	0.6	0.8	1	1.2	1.4	1.6	1.8	2
Ft_s (gf)	—	8	17	26	35	44	53	62	71	80	90
Fn_s (gf)	20	20	41	62	84	105	126	147	169	191	214
Sm_s (gf)	—	21	21	21	21	21	22	22	23	23	24
$Sm\%$	—	106	51	34	25	20	17	15	13	12	11

SMDS: safety margin derivation system.

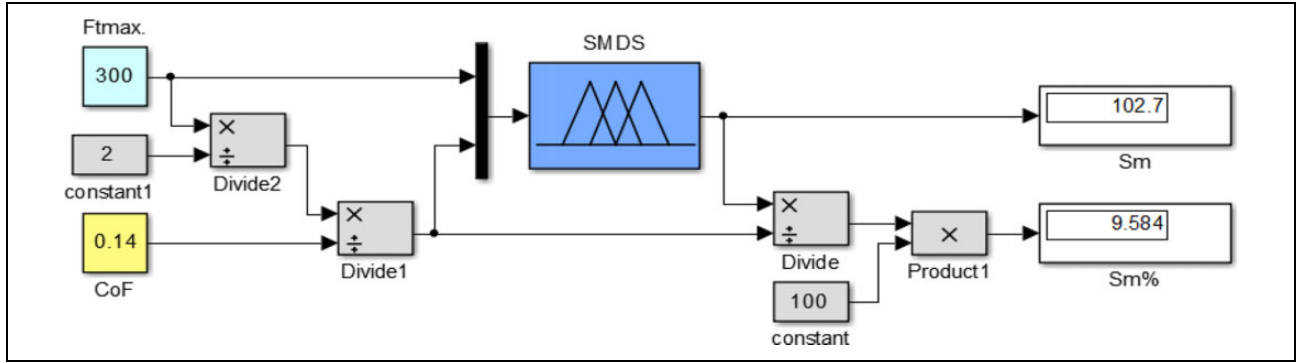


Figure 14. Matlab/Simulink model for lifting derivation performance of SMDS. SMDS: safety margin derivation system.

Table 7. Sm data of grasping performance of SMDS.

		$F_{t_{max}}$ (gf)			
		300	500	700	900
CoF	0.75	35	50	96	125
	0.55	43	62	108	151
	0.28	68	105	161	257
	0.14	103	193	257	257
	0.07	180	257	257	257

SMDS: safety margin derivation system; CoF: coefficient of variation.

Table 8. $Sm\%$ data of grasping performance of SMDS.

		$F_{t_{max}}$ (gf)			
		300	500	700	900
CoF	0.75	18	15	21	21
	0.55	16	14	17	18
	0.28	13	12	13	16
	0.14	10	11	10	8
	0.07	8	7	5	4

SMDS: safety margin derivation system; CoF: coefficient of variation.

simulation data obtained up to second of the grip process which took place in 7 s for 0.21 CoF can be seen. To compare the performance of SMDS with the data of the human performance in Tables 3 and 4, the Matlab/Simulink model seen in Figure 14 was prepared. Lifting derivation performance of SMDS for four different object weights and five different CoF values in Tables 3 and 4 was tested. The entered weight and CoF values are the values that occur when the object is lifted. Therefore, F_{t_s} value was expressed as $F_{t_{max}}$. F_{t_s} values in the model shown in Figure 11 occur by themselves throughout the simulation depending on the boot value.

In the Simulink model in Figure 14, determined F_{t_s} values are entered by the user as $F_{t_{max}}$. By assuming that each object having $F_{t_{max}}$ weight entered was lifted at the entered CoF value, 20 different lifting scenarios were examined.

Safety margin values obtained as a result of grasping performance are given in Table 7 and the safety margin rates are given in Table 8. The decimal results obtained while getting the data are rounded to the nearest integer. The performance data of SMDS obtained in Tables 7 and 8 were compared with the human performance data in Table 3. The comparison was made for the weights and surface properties used to obtain data for human performance. This comparison can be seen in Table 9.

The precision grasp performance comparison in Table 9 is graphically shown for Sm in Figure 15 and $Sm\%$ in Figure 16. When Table 9, Figure 15 and Figure 16 are

examined, it is seen that SMDS generally produces values very close to the performance of the subjects. It is seen that safety margin rate between 9% and 20% was obtained from the experimental data of human performance. From SMDS, safety margin rates between 8% and 21% were obtained.

As a result, SMDS was seen to produce optimum safety margin to grasp and lift objects according to their varying surface friction properties and varying weights by mimicking safety margin application behaviors of human beings. The obtained results reveal the usability of SMDS in the control of grip force for precision grasp task of a robotic hand.

Results and discussion

In order for a robotic hand to grasp and lift an object without causing any permanent deformation and dropping, the grip force must be controlled. In the precision grasp task of a robotic hand, the amount of grasping force that will prevent permanent deformation of an object and falling of that unknown object contains uncertainty. The purpose of this study is to control grip force with optimum safety margin for a robotic hand to precisely grasp an unknown object. There is no mathematical model related to how much the safety margin changes depending on which conditions. Therefore, in this study, the fuzzy logic method from flexible calculation methods was used.

In this study, SMDS was designed using data of safety margin performance of humans while grasping an object.

Table 9. Comparison of SMDS and human grasping performance values.

$F_{t_{max}}$ CoF		300 gf					500 gf				700 gf			900 gf		
		0.75	0.55	0.28	0.14	0.07	0.75	0.55	0.28	0.14	0.75	0.55	0.28	0.75	0.55	0.28
Sm (gf)	Human	33	46	71	111	174	51	70	105	190	81	110	160	120	165	247
	SMDS	35	43	68	103	180	50	62	105	193	96	108	161	125	151	257
Sm (%)	Human	16	17	13	11	9	15	15	12	10	17	17	13	20	20	15
	SMDS	18	16	13	10	8	15	14	12	11	21	17	13	21	18	16

SMDS: safety margin derivation system; CoF: coefficient of variation.

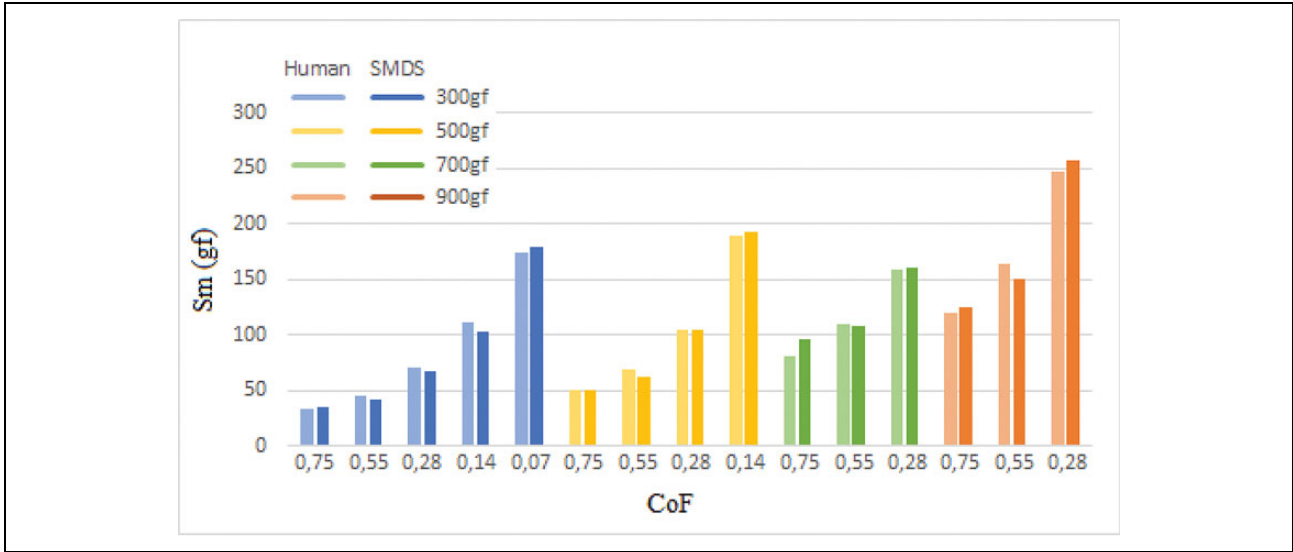


Figure 15. Comparison of SMDS and human Sm performance values. SMDS: safety margin derivation system.

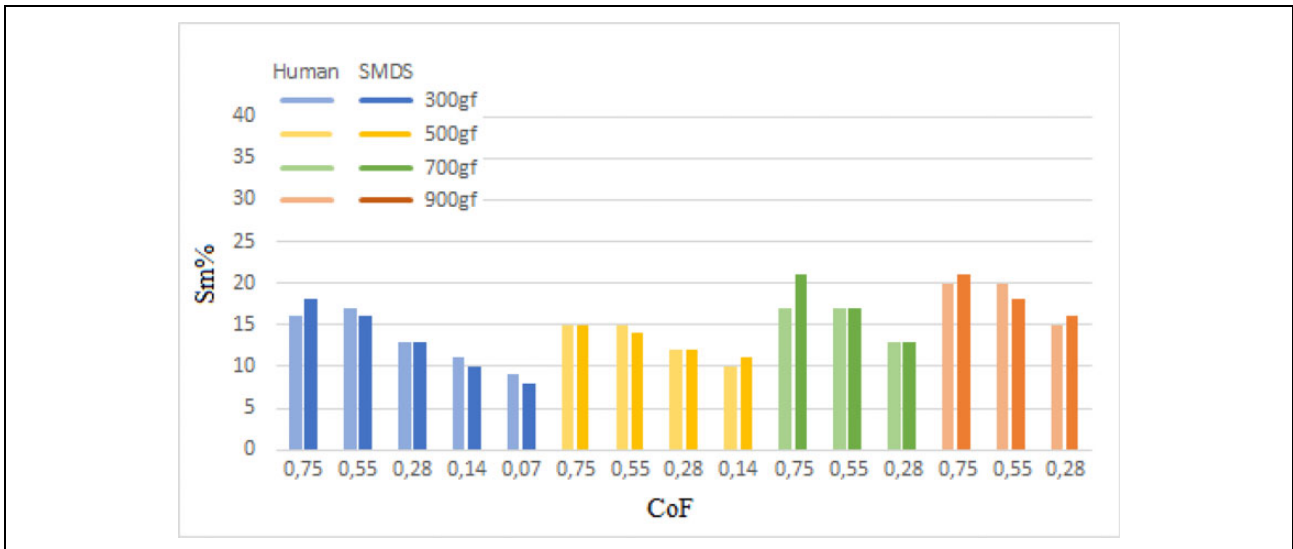


Figure 16. Comparison of SMDS and human Sm% performance values. SMDS: safety margin derivation system.

With the designed SMDS, the optimum safety margin of a robotic hand in precision grasp task was calculated. Safety margin derivations and safety margin percentage rates of grasping and lifting performances of SMDS that were

designed and simulated in the Matlab environment, according to varying surface properties and varying weights, were obtained. The obtained data were compared with human performance and the results were examined. The results

of this study were obtained for 300 and 900 gf weight value range and 0.07 and 0.75 coefficient of static friction range depending on soft fingertip contact model and two-finger precision grasp model in which thumb and index fingers were used. It is assumed that only normal force affects the grasped object on horizontally and tangential force affects in a vertical direction. In the conducted performance comparison, it was seen that SMDS provided safety margin derivations very close to human performance according to varying conditions. It was seen that safety margin rates of 9% and 20% were obtained from the experimental tests conducted for human performance depending on varying surface properties and varying weight.

The obtained results reveal the usability of SMDS for the control of grasping force in precision grasp task of a robotic hand of SMDS. SMDS can be optimized by measuring human's safety margin performances under different conditions and different combined force effects. In addition, the performance of grasping force control can be increased with SMDS in models, where local partial slips are evaluated such as stick-slip friction model.


Declaration of conflicting interests


The author(s) declared no potential conflicts of interest with respect to the research, authorship, and/or publication of this article.

Funding

The author(s) disclosed receipt of the following financial support for the research, authorship, and/or publication of this article: This work was supported in part by the Mustafa Kemal University Scientific Research Projects Coordinator ship under grant no. 9861.

ORCID iD

Canfer Islek  <https://orcid.org/0000-0001-9728-8431>

Ersin Ozdemir  <https://orcid.org/0000-0002-6598-9484>

References

- Cutkosky MR. On grasp choice, grasp models, and the design of hands for manufacturing tasks. *IEEE Trans Robot Autom* 1989; 5(3): 269–279.
- Mavrakis N, Ghalamzan EAM, and Stolkin R. Safe robotic grasping: minimum impact-force grasp selection. In: *2017 IEEE/RSJ international conference on intelligent robots and systems (IROS)*, Vancouver, BC, Canada, 24–28 September 2017, pp. 4034–4041. IEEE.
- Cutkosky MR and Howe RD. Human grasp choice and robotic grasp analysis. In: Venkataraman ST and Iberall T (eds) *Dexterous robot hands*, New York, NY: Springer, 1990, pp. 5–31.
- Tremblay MR, Packard WJ, and Cutkosky MR. Utilizing sensed incipient slip signals for grasp force control. In: *Proc. Japan-USA symposium on flexible automation*, San Francisco, CA, USA, 13–15 July 1992, pp. 1–6.
- Tremblay MR and Cutkosky MR. Estimating friction using incipient slip sensing during a manipulation task. In: *Proc. IEEE international conference on robotics and automation*, Atlanta, GA, USA, 2–6 May 1993, pp. 429–434. IEEE.
- Dubey VN, Crowder RM, and Chappell PH. Optimal object grasp using tactile sensors and fuzzy logic. *Robotica* 1999; 17(6): 685–693.
- Glossas NI and Aspragathos NA. Fuzzy logic grasp control using tactile sensors. *Mechatronics* 2001; 11(7): 899–920.
- Dominguez-López JA, Damper RI, Crowder RM, et al. Optimal object grasping using fuzzy logic. In: *Proc. international conference on robotics, vision, information and signal processing (ROVISP'2004)*, Penang, Malaysia, 1 January 2003, pp. 367–372.
- Maeno T, Kawamura T, and Cheng SC. Friction estimation by pressing an elastic finger-shaped sensor against a surface. *IEEE Trans Robot Autom* 2004; 20(2): 222–228.
- Ikeda A, Kurita Y, Ueda J, et al. Grip force control for an elastic finger using vision-based incipient slip feedback. In: *Proc. 2004 IEEE/RSJ international conference on intelligent robots and systems (IROS)*, Sendai, Japan, 28 September–2 October 2004, pp. 810–815. IEEE.
- Koda Y and Maeno T. Grasping force control in master-slave system with partial slip sensor. In: *Proc. 2006 IEEE/RSJ international conference on intelligent robots and systems*, Beijing, China, 9–15 October 2006, pp. 4641–4646. IEEE.
- O'Toole M, Bouazza-Marouf K, Kerr D, et al. Robust contact force controller for slip prevention in a robotic gripper. *Proc Inst Mech Eng Part I: J Syst Control Eng* 2010; 224(3): 275–288.
- Ho VA and Hirai S. Understanding slip perception of soft fingertips by modeling and simulating stick-slip phenomenon. In: *Proc. robotics: science and systems VII*, Los Angeles, CA, USA, 27–30 June 2011, pp. 129–136.
- Yuan W, Li R, Srinivasan MA, et al. Measurement of shear and slip with a GelSight tactile sensor. In: *Proc. 2015 IEEE international conference on robotics and automation (ICRA)*, Seattle, WA, USA, 26–30 May 2015, pp. 304–311. IEEE.
- Lu Y, Zhang C, Cao C, et al. Analysis of coordinated grasping kinematics and optimization of grasping force of a parallel hybrid hand. *Int J Adv Robot Syst* 2017; 14(3): 1–14.
- Morita N, Nogami H, Higurashi E, et al. Grasping force control for a robotic hand by slip detection using developed micro laser doppler velocimeter. *Sensors* 2018; 18(2): 326.
- Pettersson-Gull P and Johansson J. *Intelligent robotic gripper with adaptive grasp technique*. MS Thesis, Mälardalen University, Sweden, 2018.
- Calandra R, Owens A, Jayaraman D, et al. More than a feeling: Learning to grasp and regrasp using vision and touch. *IEEE Robot Autom Lett* 2018; 3(4): 3300–3307.
- Johansson RS and Westling G. Roles of glabrous skin receptors and sensorimotor memory in automatic control of precision grip when lifting rougher or more slippery objects. *Exp Brain Res* 1984; 56(3): 550–564.

20. Edin BB, Westling G, and Johansson RS. Independent control of human finger-tip forces at individual digits during precision lifting. *J Physiol* 1992; 450(1): 547–564.
21. Hadjiosif AM and Smith MA. Flexible control of safety margins for action based on environmental variability. *J Neurosci* 2015; 35(24): 9106–9121.
22. Wettels N, Parnandi AR, Moon JH, et al. Grip control using biomimetic tactile sensing systems. *IEEE/ASME Trans Mechatron* 2009; 14(6): 718–723.
23. Johansson RS and Flanagan JR. Tactile sensory control of object manipulation in humans. In: Gardner E and Kaas JH (eds) *The senses: a comprehensive reference, vol.: somatosensation*. Amsterdam: Elsevier, 2008, pp. 67–86.
24. Wiertlewski M, Endo S, Wing AM, et al. Slip-induced vibration influences the grip reflex: a pilot study. In: *Proc. 2013 world haptics conference (WHC)*, Daejeon, South Korea, 14–17 April 2013, pp. 627–632. IEEE.
25. Su Z, Hausman K, Chebotar Y, et al. Force estimation and slip detection/classification for grip control using a biomimetic tactile sensor. In: *Proc. 2015 IEEE-RAS 15th international conference on humanoid robots (humanoids)*, Seoul, South Korea, 3–5 November 2015, pp. 297–303. IEEE.
26. Hiramatsu Y, Kimura D, Kadota K, et al. Control of precision grip force in lifting and holding of low-mass objects. *PLoS one* 2015; 10(9): e0138506.
27. Islek C and Özdemir E. Robot elin hassas kavrama görevi için bulanık mantık ile kavrama kuvvetinin kontrolü. In: *Proc 2019 international engineering and science symposium (IESS)*, Siirt, Turkey, 20–22 June 2019, pp. 1041–1047.
28. Zhang H, Alrifai M, Zhou K, et al. A novel fuzzy logic algorithm for accurate fall detection of smart wristband. *Trans Inst Meas Control* 2020; 42(4): 786–794.
29. Zadeh LA. Fuzzy sets. *Inform Control* 1965; 8(3): 338–353.
30. Rodrigue RM, Martinez L, and Herrera F. Hesitant fuzzy linguistic term sets for decision making. *IEEE Trans Fuzzy Syst* 2012; 20(1): 109–119.
31. Kocabaş A. Design and optimization of a fuzzy logic based maximum power point tracker for PV panel. M.S Thesis, Karadeniz Technical University, Turkey, 2017.
32. Tüysüz M. Hibrit güç sistemlerinde maksimum güç noktası takibi için bulanık denetleyicinin optimizasyonu. MS Thesis, Karadeniz Technical University, Turkey, 2018.
33. Tari E. Ölü zamanlı sistemlerde üyelik fonksiyonlarının taban aralığının ayarlanmasına dayalı bulanık kontrolör tasarımı. MS Thesis, Istanbul Technical University, Turkey, 2010.
34. Reisi AR, Moradi MH, and Jamasb S. Classification and comparison of maximum power point tracking techniques for photovoltaic system: a review. *Renew Sustain Energ Rev* 2013; 19: 433–443.
35. Mamdani EH and Assilian S. An experiment in linguistic synthesis with a fuzzy logic controller. *Int J Hum-Comput Stud* 1999; 51(2): 135–147.
36. Cheng J, Xu M, and Chen Z. A fuzzy logic-based method for risk assessment of bridges during construction. *J Harbin Inst Technol (New Series)* 2019; 26(1): 1–10.